AGU
ADVANCING EARTH AND SPACE SCIENCE

# Geophysical Research Letters®

**Key Points:**

- Coupled Model Intercomparison Project Phase 6 (CMIP6) large ensembles allow the relationship between climate sensitivity and response to volcanic eruptions to be investigated
- The climate response to the eruption of Mt. Pinatubo does not correlate well with equilibrium climate sensitivity (ECS) across CMIP6 models
- Previous claims that the response to Pinatubo could constrain ECS are consistent with statistical chance

# The Climate Response to the Mt. Pinatubo Eruption Does Not Constrain Climate Sensitivity

Andrew G. Pauling[1] [ID], Cecilia M. Bitz[1] [ID], and Kyle C. Armour[1,2] [ID]

[1]Department of Atmospheric Sciences, University of Washington, Seattle, WA, USA, [2]School of Oceanography, University of Washington, Seattle, WA, USA

**Abstract** The climate response to the Mt. Pinatubo volcanic eruption is analyzed using large ensembles of Coupled Model Intercomparison Project Phase 6 (CMIP6) historical simulations. In contrast to previous work, we find that standard measures of the global temperature response to volcanic forcing are not significantly correlated with climate sensitivity across models. Isolating the shortwave response due to non-cloud effects does not improve the correlation with climate sensitivity. Earlier constraints on climate sensitivity based on the response to Mt. Pinatubo are consistent with having arisen by chance because of the small size of the ensembles used. Our results suggest that the response to Mt. Pinatubo cannot be used to constrain the climate sensitivity to increased greenhouse gas concentrations, as has been proposed, because the radiative feedbacks in response to volcanic eruptions are not well correlated with the feedbacks governing the long-term response to greenhouse gas forcing.

**Plain Language Summary** Large volcanic eruptions influence climate by injecting sulfate aerosols into the stratosphere. It has been proposed that the response of the climate system to recent large eruptions can inform estimates of current and anticipated climate change driven by increasing levels of carbon dioxide in the atmosphere by comparing the simulated temperature responses driven by the two types of forcing across a variety of climate models. Here we show that numerous simulations are necessary to quantify the variability of the climate response to recent volcanic eruptions, and taken together the simulations show that the proposed relationship does not exist. Thus volcanic eruptions do not constrain 21st century climate change, and the results of earlier studies are consistent with having arisen by chance owing to the reduced number of simulations that were available. We propose that the lack of relationship is because climate feedbacks differ when driven by volcanic eruptions versus increased carbon dioxide.

## 1. Introduction

Large volcanic eruptions can influence global climate through the injection of sulfate aerosols into the stratosphere (e.g., Robock, 2000). Eruptions occurring in the tropics, in particular, can influence climate globally as the aerosols can be dispersed by the Brewer-Dobson circulation to high latitudes in both hemispheres. The eruption of Mt. Pinatubo in June 1991 resulted in distribution of aerosols roughly symmetrically between the two hemispheres, and provides a useful natural case study of a global-scale radiative forcing that is not due to anthropogenic greenhouse gas emissions. The utility of studying the climate response to Mt. Pinatubo has been noted before (e.g., Bender et al., 2010; Robock, 2000; Soden et al., 2002), and it has been argued that it can be used to constrain the equilibrium climate sensitivity (ECS) (Bender et al., 2010; Forster et al., 2021).

ECS is typically defined as the steady-state global-mean surface temperature (GMST) change in response to a doubling of the atmospheric $CO_2$ concentration relative to pre-industrial levels. It was estimated to fall within the *likely* range 1.5°C–4.5°C by the report of Charney et al. (National Research Council, 1979). More recently, the *likely* range was assessed to be 2.5°C–4°C by the Intergovernmental Panel on Climate Change Sixth Assessment Report (IPCC AR6, Forster et al., 2021). This narrowing of the ECS range was in large part achieved by consideration of *emergent constraints* (e.g., Eyring et al., 2019; Hall et al., 2019; Klein & Hall, 2015), a term which describes the practice of identifying a relationship between some physical quantity and ECS across climate models, and using the derived relationship to calculate a range for the observed ECS from the observed physical quantity. The relationship is typically obtained by using many different climate model simulations.

One emergent constraint used in IPCC AR6 was that of Bender et al. (2010) who proposed that the climate response to the Mt. Pinatubo eruption might provide a constraint on ECS. The proposal hinges on the assumption

that climate feedbacks under volcanic forcing are correlated with those under $CO_2$ forcing and that this correlation is accurately represented by climate models. Bender et al. (2010) defined the *volcanic sensitivity* as the ratio of the time-integrated GMST response to the time-integrated top-of-atmosphere reflected shortwave (TOA reflected SW) radiative flux response averaged over the tropics (20°S–20°N) following the Mt. Pinatubo eruption. In historical simulations in the Coupled Model Intercomparison Project Phase 3 (CMIP3), they found a linear relationship between volcanic sensitivity and ECS after eliminating one outlier model among the 10 available that included volcanic forcing. They then used the observed volcanic sensitivity to constrain ECS to lie within the 5%–95% confidence range of 1.7°C–4.1°C.

There were only nine models that participated in CMIP3 that were identified by Bender et al. as suitable for computing the volcanic responses detailed above, with a total of 23 ensemble members. In the Coupled Model Intercomparison Project Phase 6 (CMIP6), there are now 16 models with at least 10 ensemble members for their historical simulations, giving a total of 543 ensemble members. This much greater quantity of model output offers an opportunity to evaluate the robustness of the constraint found by Bender et al. (2010). In this paper we make use of this model output to examine whether the constraint on climate sensitivity is reliable, given the potential for correlations to arise by chance within model ensembles (e.g., Caldwell et al., 2014; Hall et al., 2019; Klein & Hall, 2015). The large volume of model output also allows us to better evaluate the role of internal variability in the climate response to volcanic eruptions.

## 2. Data and Methods

We analyze output from the 16 models that participated in CMIP6 with at least 10 ensemble members of historical (1850–2014) simulations (see Supporting Information S1). We also include the recent CESM2 Large Ensemble (CESM2-LE, Rodgers et al., 2021), which has 100 ensemble members over the historical period and uses the same historical forcing protocol as the CMIP6 models, except half of the ensemble members use slightly different prescribed biomass burning emissions. Over the period in which the eruption of Mt. Pinatubo occurred, the stratospheric aerosols in the historical simulations are prescribed from the climatology of Thomason et al. (2018).

Following Bender et al. (2010) we quantify the response to the Mt. Pinatubo eruption in the CMIP6 historical simulations from anomalies of various quantities relative to their monthly climatology over the reference period January 1986–December 1990. To remove the long-term trend from increasing greenhouse gases, we remove the linear trend from the anomalies from January 1986 to December 2005. When calculating the linear trend we exclude the data between June 1991 and May 2001 to remove only the linear trend due to increasing greenhouse gas concentrations without including the influence from the volcanic eruption in the trend. We compute correlations between variables across the CMIP6 models using the Pearson correlation coefficient. All correlations are computed using ensemble mean quantities for each model to reduce the influence of internal variability.

We compare the CMIP6 models' tropical-mean (20°S–20°N) TOA reflected SW radiative flux response to the Mt. Pinatubo eruption to data from the Earth Radiation Budget Experiment (ERBE, Barkstrom, 1984) Wide-Field-Of-View Nonscanner Observations version 4.1 (NASA/LARC/SD/ASDC, 2020). This data set provides TOA radiative fluxes measured from the satellite over the period January 1985–December 1999, averaged over 36-day periods. Due to the missing data in the record between July 1993 and January 1994, after which there is a substantial offset and increased variability, we only use the data up to June 1993. For GMST we evaluate CMIP6 models with the HadCRUT5 data set (Morice et al., 2021).

To investigate the role of clouds in the climate response among CMIP6 models, we isolate the monthly TOA radiative flux anomalies due to non-cloud effects using the Approximate Partial Radiative Perturbation (APRP) method of Taylor et al. (2007).

The studies of Held et al. (2010) and Gregory et al. (2016) showed that the magnitude of the climate response to episodic forcing like volcanic eruptions depends strongly on the amount of ocean heat uptake (OHU) following the eruption. To test whether this relationship holds among CMIP6 models, we compute OHU using monthly-mean net surface radiative fluxes, turbulent fluxes, and latent heat from melting snow.

We estimate ECS and the corresponding climate feedback parameter $\lambda$ for CMIP6 models from the Gregory et al. (2004) regression method by obtaining the $x$-intercept as an estimate of the equilibrium GMST response to quadrupling $CO_2$ and the slope as an estimate of $\lambda$. Half the equilibrium GMST provides an estimate of

ECS (Zelinka et al., 2020, values of ECS for each model were obtained from the Zenodo repository https://doi.org/10.5281/zenodo.5206851). Note that values of ECS diagnosed by this method are only an approximation of the true ECS, which might be slightly different depending on how radiative feedbacks evolve on longer timescales (e.g., Rugenstein et al., 2020; Sherwood et al., 2020).

To gain intuition for the expected relationship between the climate response to a volcanic eruption and ECS, we use the two-layer energy balance model of Held et al. (2010). The model simulates an upper and deep ocean temperature when subject to a radiative forcing with four free parameters. We calibrate the parameters so the upper-ocean layer mimics the GMST of a particular CMIP6 model in response to increasing $CO_2$, repeating so that each CMIP6 model is associated with a unique parameter set. One of the parameters is the climate feedback parameter $\lambda$, computed as described above. The other three free parameters are fit using the procedure described in Geoffroy et al. (2013) (see Supporting Information S1). This method has previously been used in the study of emergent constraints with CMIP6 model output (Nijsse et al., 2020). Once we have the parameter set associated with each CMIP6 model, we use the two-layer model to compute an idealized GMST response ($T_{2l}$) to the Mt. Pinatubo eruption for each CMIP6 model using an estimate of the radiative forcing from Schmidt et al. (2018). Importantly, climate feedbacks within the two-layer model are prescribed to be the same for a volcanic eruption and increasing $CO_2$.

We also use the two-layer model to compute an idealized TOA SW radiative flux response to the Mt. Pinatubo eruption. We first obtain the SW radiative feedback parameter $\lambda_{SW}$ as we did for $\lambda$, but with the TOA SW radiative flux imbalance rather than the total net radiative flux imbalance in the regression. We then compute the idealized TOA SW radiative flux response to the eruption as $\lambda_{SW}T_{2l}$.

## 3. Results

The GMST response to the Mt. Pinatubo eruption is reproduced well in CMIP6 historical simulations, with observed peak cooling of about 0.4 K relative to the reference period (1986–1990) falling within the spread of the models (Figure 1a). The observed peak SW anomaly of about $-9$ W m$^{-2}$ is larger than that in any of the CMIP6 models, which mostly peak around $-6$ W m$^{-2}$ (Figure 1b). In both models and observations the peak cooling occurs about a year after the eruption. We find no statistically significant correlation across models between the peak SW response and the peak temperature response.

As noted by Bender et al. (2010), the TOA reflected SW flux anomaly has contributions from both the SW radiative forcing from the volcano-derived sulfate aerosols and SW radiative response to global cooling. Also, despite the SW forcing being the dominant contributor to the total radiative forcing from volcanic eruptions (Schmidt et al., 2018), there is a substantial component from longwave forcing. Following Bender et al. (2010), we use the TOA reflected SW flux anomaly in lieu of radiative forcing due to many modeling centers not running the fixed-SST experiments (with only volcanic forcing) that would be necessary to compute the effective radiative forcing due to the eruption of Mt. Pinatubo. The spread in the TOA reflected SW response to the volcanic eruption (Figure 1b) could be due to spread in the SW radiative forcing or the spread in SW radiative response. Some of the models used in our analysis (CNRM-CM6-1, CanESM5, GISS-E2-1-G, IPSL-CM6A-LR, and MIROC6) ran the piClim-histnat experiment from the Radiative Forcing Model Intercomparison Project (Pincus et al., 2016), which uses only natural climate forcing (e.g., solar forcing and volcanic eruptions) over the historical period, with SSTs prescribed from the climatology of a long-term pre-industrial control run of the model. We computed the peak SW radiative forcing in each of the models for which the piClim-histnat experiment was available (not shown), and found that the standard deviation is about 0.18 W m$^{-2}$. Because the standard deviation of the peak SW flux anomaly in Figure 1a is much larger, 1.33 compared to 0.18 W m$^{-2}$, the spread in the TOA reflected SW anomaly for individual model's ensemble means is dominated by the spread in the forced response to the volcanic eruption. A key question, then, is whether the response to Pinatubo can be used to constrain ECS.

We first examine the relationships between ECS and idealized estimates of the time-integrated GMST response, the time-integrated TOA SW response, and the volcanic sensitivity ratio, obtained from the Held et al. (2010) two-layer model with the model parameters derived from increasing $CO_2$ in each CMIP6 model. The correlations obtained when we ran the two-layer model with volcanic forcing are $r = -0.81$ for GMST, $r = 0.70$ for TOA SW and $r = -0.75$ for the volcanic sensitivity ratio of the integrated GMST to the integrated TOA SW flux anomaly (correlations illustrated by lines in Figure 2). These relatively high correlations suggest that we should expect to
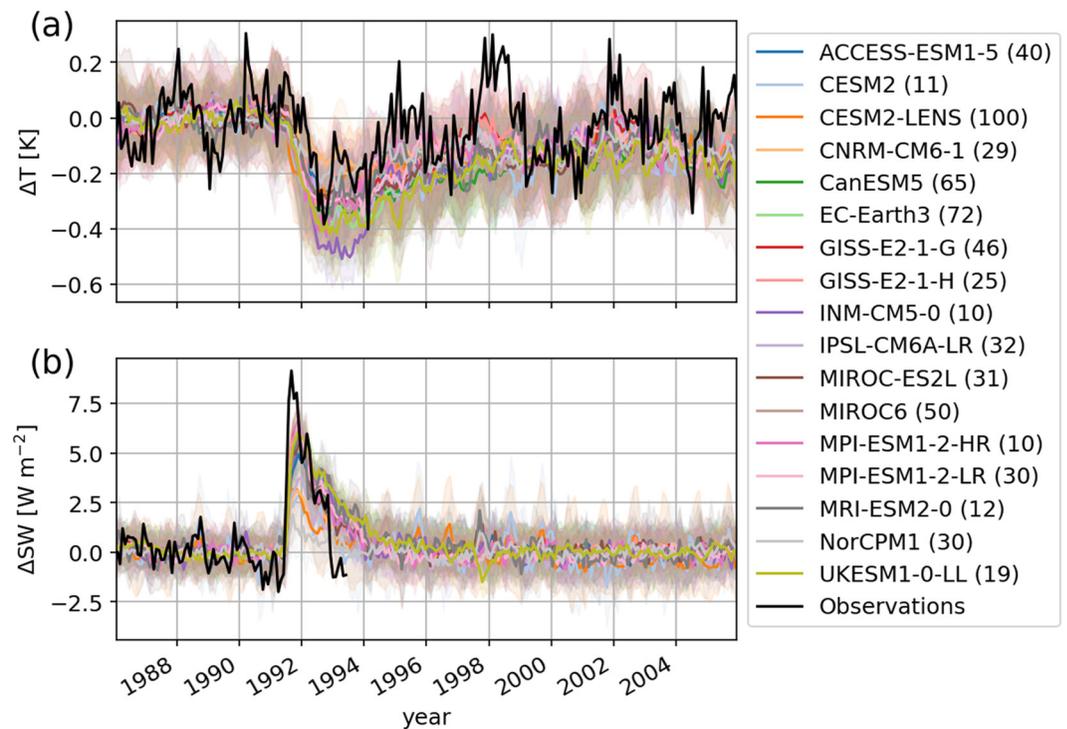
**Figure 1.** (a) Global-mean surface temperature and (b) top-of-atmosphere reflected shortwave radiative flux anomalies in response to the Mt. Pinatubo eruption in Coupled Model Intercomparison Project Phase 6 historical simulations and observations. Lines are the ensemble mean of each model and shading denotes $\pm 1$ standard deviation from the ensemble mean. Black lines show the observed quantities from the Earth Radiation Budget Experiment satellite and HadCRUT5 data for $\Delta$SW and $\Delta$T, respectively. Numbers in parentheses in the legend denote the number of ensemble members for each model.
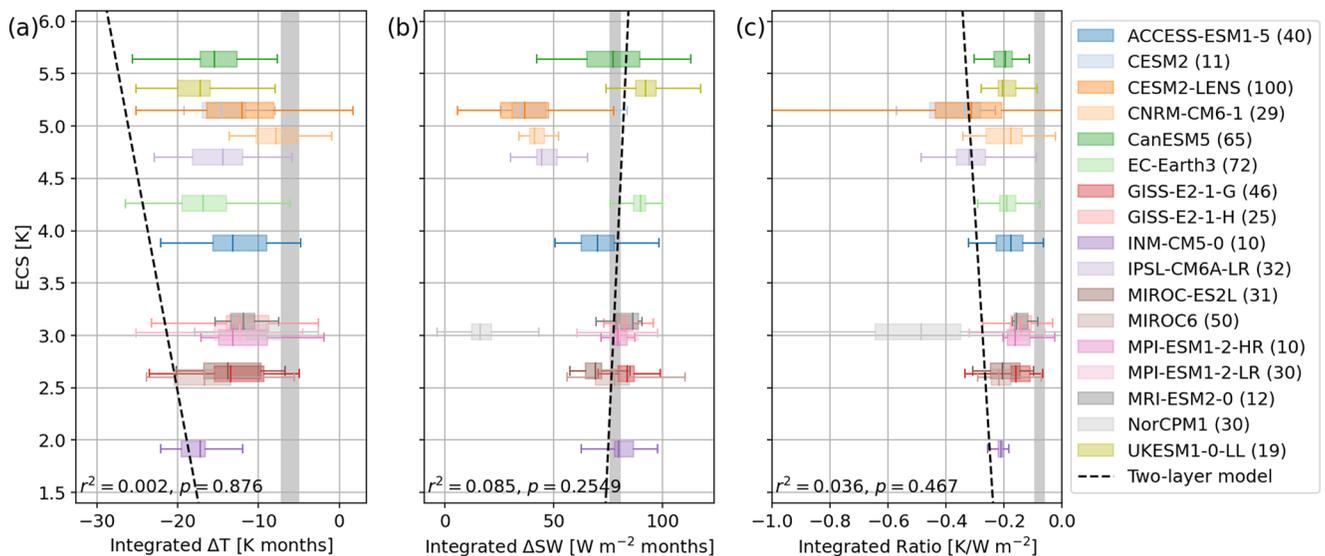


**Figure 2.** (a) Integrated global-mean surface temperature (GMST) response (averaged June 1991–May 1996), (b) integrated top-of-atmosphere (TOA) reflected shortwave (SW) radiative flux response (averaged 20°S–20°N and June 1991–May 1993), and (c) volcanic sensitivity versus equilibrium climate sensitivity (ECS). The $r^2$ and $p$-values for the correlation are shown in the bottom left corner of each panel. The gray shaded regions show the range of observed values obtained by integrating the TOA reflected SW radiative flux response 18–24 months and integrating the GMST response 4–6 years. The black dashed lines show the regression line for idealized responses estimated from the two-layer energy balance model for the quantities on the $x$-axis and ECS. A regression line that is not vertical indicates that we should expect a relationship between the quantities assuming the feedbacks are the same as those for increased $CO_2$. Numbers in parentheses in the legend denote the number of ensemble members for each model.

see a correlation between the response to volcanic eruptions and ECS if the feedbacks in each model are the same in response to volcanic eruptions as to increased $CO_2$. Do CMIP6 models produce similar correlations?

Following Bender et al. (2010), we analyze time-integrated GMST and TOA reflected SW fluxes, but in the much larger quantity of model output available today. We integrate over the same time periods used in Bender et al. (2010): June 1991–May 1996 for temperature and June 1991–May 1993 for TOA reflected SW. Consistent with their results, we find no relationship between ECS and the time-integrated GMST anomaly (Figure 2a). We also do not find a statistically significant linear relationship between ECS and the time-integrated TOA reflected SW flux anomaly (Figure 2b). However, in contrast to the findings of Bender et al. (2010), we find no statistically significant linear relationship between ECS and the volcanic sensitivity ratio (Figure 2c). That is, the basis for the Bender et al. (2010) emergent constraint on ECS does not appear to be robust when evaluated using CMIP6 models. Bender et al. (2010) quantified the uncertainty in their estimates of the volcanic sensitivity by varying the length of time over which the anomalies were integrated. However, it is not obvious that this approach captures the true uncertainty due to internal variability in the climate system. The spread across ensemble members of large ensembles of climate model integrations approximately represents spread due to internal climate system variability. The spread across ensemble members for each model in Figure 2 shows that internal variability is much larger than the spread due to varying the integration time. Moreover, the spread across ensemble members in the quantities shown in Figure 2 spans the intermodel differences among models. Such a large role for internal variability in the response to volcanic eruptions suggests that caution would be needed in the use of Pinatubo as an emergent constraint even if robust relationships between observable quantities and ECS could be found.

The correlations between ECS and either the integrated temperature response or the volcanic sensitivity ratio found within CMIP6 models are substantially lower than those found using the two-layer model (Figures 2a and 2c). This suggests that the radiative feedback parameter obtained from abrupt-4xCO2 experiments does not characterize the feedback due to volcanic forcing well, as has been previously suggested by Merlis et al. (2014) and Ceppi and Gregory (2019). This could be due to differences in the feedback due to the fundamentally different physical nature of the forcing, the spatial pattern of the temperature response to the volcanic eruption resulting in a different TOA radiative flux response to the same global mean forcing, or a combination of the two. To diagnose whether the differing feedbacks can be attributed to warming versus cooling scenarios, we fit the parameters of the two-layer model using the response to either abruptly quadrupling or abruptly halving atmospheric $CO_2$ (see Supporting Information S1). We found that using the parameters fit to the cooling scenario did not systematically improve the two-layer model's ability to reproduce the CMIP6 model response, indicating that the difference in feedbacks is not simply due to a difference between warming and cooling scenarios.

Given these results, it is worth considering what led to the correlation between the volcanic sensitivity ratio and ECS in Bender et al. (2010). One possibility is that some aspect of the models in CMIP3 caused an apparent relationship between the two quantities to occur that, due to model developments, no longer occurs in CMIP6, casting doubt on the validity of the physical relationship and its use as an emergent constraint on ECS.

Another possibility is that the correlation identified by Bender et al. (2010) arose by chance given internal variability in the climate system. To quantify how likely it is to obtain the relationship shown in Bender et al. (2010) by chance, we randomly chose 23 ensemble members from nine CMIP6 models (three members for seven of the models and one member from two models, which is all that was available among the nine models used in the Bender et al. (2010) study) and compute the linear relationship between ECS and volcanic sensitivity (Supporting Information S1). We fit the histogram of regression slopes with a Student t-distribution which gave a mean slope of $-0.010$ (W m$^{-2}$)$^{-1}$ and a standard deviation of 0.014 (W m$^{-2}$)$^{-1}$. The slope computed from the CMIP3 model output used by Bender et al. (2010) falls within this distribution, but the spread of the slopes obtained from the CMIP6 model output highlights that it was possible that they could have found a regression slope greater than zero. Thus, the strong correlation between volcanic sensitivity and climate sensitivity found by Bender et al. (2010) may have arisen due to statistical chance resulting from the relatively small number of ensemble members (23) in the CMIP3 output as compared to the CMIP6 output (543).

## 3.1. Non-Cloud Volcanic Sensitivity and Ocean Heat Uptake

As noted above, the TOA SW flux anomaly reflects a combination of radiative forcing (interaction of stratospheric aerosols with SW radiation) and the SW radiative response to global cooling. It is thus possible that any
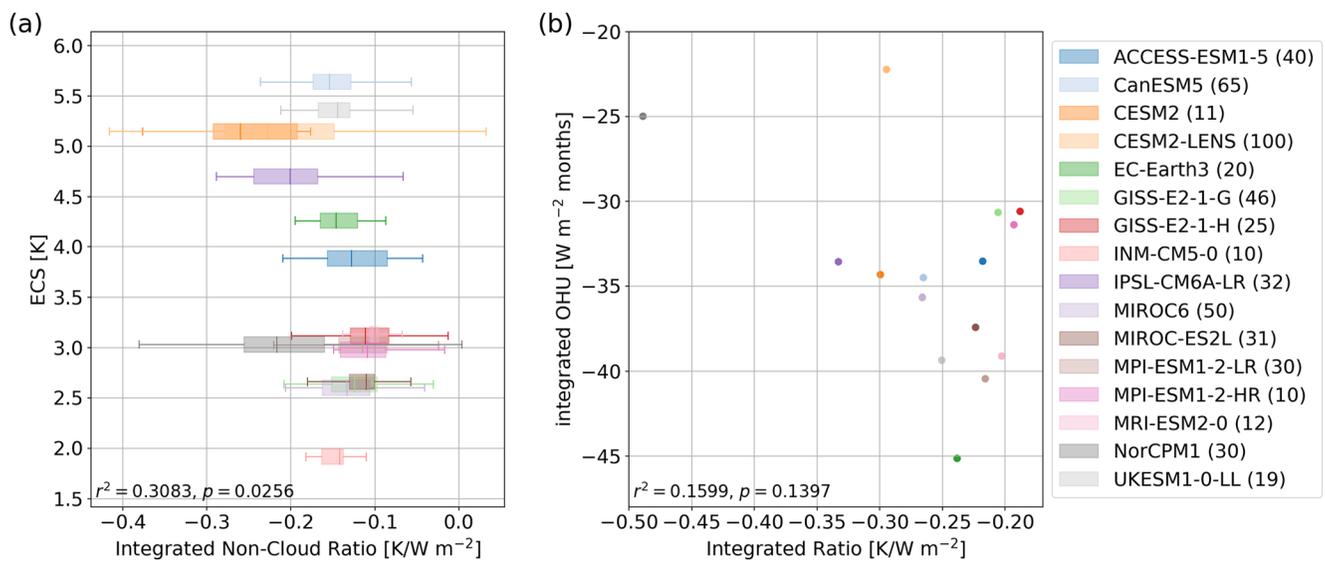
**Figure 3.** (a) Equilibrium climate sensitivity versus non-cloud volcanic sensitivity following the eruption of Mt. Pinatubo. (b) Time-integrated ocean heat uptake (over the period June 1991–May 1993) versus volcanic sensitivity for each of the models analyzed. The $r^2$ value and $p$-value for each correlation are shown at the bottom of each panel. Numbers in parentheses in the legend denote the number of ensemble members for each model.

underlying correlation between volcanic sensitivity and ECS is obscured by the influence of radiative feedbacks on the TOA SW flux. To decompose these factors, we next repeat the analysis shown in Figure 2 while making use of the approximate partial radiative perturbation (APRP, Taylor et al., 2007) method to remove the portion of the TOA SW flux anomaly that is due to the cloud response (Figure 3). The non-cloud component of the TOA SW flux should be mostly due to the interaction of aerosols with SW radiation, which is the dominant direct impact of a volcanic eruption and larger than SW changes associated with surface albedo in response to the resulting cooling. The non-cloud component of the TOA SW flux is thus a better measure of the volcanic radiative forcing. We then use this non-cloud component of the TOA SW flux to compute the *non-cloud volcanic sensitivity*, defined as the ratio of the time-integrated 2 m air temperature anomaly over the period June 1991–May 1996 to the time-integrated non-cloud component of the TOA SW flux anomaly over the period June 1991–May 1993.

There is a small but statistically significant ($p < 0.05$) correlation between the non-cloud volcanic sensitivity and ECS (Figure 3a). This relationship only explains ∼32% of the variance across all ensemble members. The relatively small fraction of the variance explained by this relationship indicates that the non-cloud volcanic sensitivity is a poor constraint on ECS. That both the TOA SW anomaly and its non-cloud component (a more direct measure of the volcanic radiative forcing) show little relationship with ECS suggests that the differing impact of cloud radiative responses to temperature changes among models is not obscuring an underlying relationship between the response to the volcanic eruption and ECS.

So far we have only examined radiative fluxes at the TOA in response to the eruption of Mt. Pinatubo. However, differences in the temperature response to volcanic forcing may also arise from differences in OHU (i.e., the net surface flux). The OHU response to the volcanic eruption is negative indicating a heat flux from the ocean to the atmosphere since it is a response to negative forcing and cooling. We find no statistically significant relationship between the integrated OHU and the GMST response (Figure 3b). This indicates that differing changes in OHU across model are not masking a relationship between ECS and the volcanic sensitivity.

## 4. Discussion and Conclusions

We find that the CMIP6 models used in this study reproduce well the observed GMST and underestimate the observed TOA reflected SW flux anomalies following the eruption of Mt. Pinatubo. Similar to the results of Bender et al. (2010), we find no relationship between either the time-integrated GMST response or the time-integrated tropical-mean TOA reflected SW response and ECS. However, in contrast to their results we also find no relationship between the volcanic sensitivity ratio and ECS. We find that the strong correlation found

by Bender et al. (2010) may be the result of statistical chance due to the relatively small number of models and ensemble members available to them from CMIP3 output. The limited model output available in CMIP3 led to an underestimate of the role of internal variability and, with the much larger volume of model output available from CMIP6, the large spread in the response to Mt. Pinatubo, particularly in the SW response, becomes evident. In light of this result, it is evident that even if a correlation between ECS and volcanic sensitivity exists, the internal variability of the response to Pinatubo is too large to meaningfully constrain ECS.

Due to the much larger amount of model output now available we were also able to directly analyze several aspects of the climate system response to the eruption of Mt. Pinatubo that Bender et al. (2010) noted they were unable to do due to the limited output available from CMIP3. We showed that the time-integrated OHU response explains very little of the variance across all ensemble members in the time-integrated GMST response. While previous studies have shown that the OHU response is crucial for determining the magnitude of cooling following a volcanic eruption (Gregory et al., 2016; Held et al., 2010), these results show that it does not explain the spread in the response across models. We also found no relationship between ECS and the ratio of the time-integrated GMST response to the time-integrated volcanic radiative forcing computed from the piClim-histnat experiments from CMIP6 (not shown). Our analysis highlights the value of both the large volume and comprehensive nature of the climate model output from CMIP6.

These results also raise the question: what aspect of the climate system does control the response to volcanic eruptions? The results of this study have shown it is not the model ECS or the feedback parameter as calculated from abrupt quadrupling of $CO_2$. Nor does OHU control the response. The recent studies of Gregory et al. (2020) and Günther et al. (2022) may shed some light on what controls the response to an eruption.

Gregory et al. (2020) computed the time-varying feedback parameter from historical simulations and showed that the feedback is more negative (effective climate sensitivity is lower) during periods affected by volcanic eruptions than during periods with greenhouse gas forcing alone. Günther et al. (2022) ran model simulations with time-invariant stratospheric sulfate aerosol forcing (SSAF) and found that in the first 10 years the feedback parameter is more negative in response to SSAF than in response to changes in $CO_2$, after which it converges toward the same value as that for $CO_2$. Günther et al. (2022) attributed this more negative short time-scale feedback parameter to greater temperature changes in the Pacific warm pool region (30°S–30°N, 50°E–160°W), a region in which temperature changes project onto strong negative feedbacks (e.g., Dong et al., 2019). They defined a "warm pool index" (WPI) to quantify the amount of temperature change in the warm pool region relative to the global mean.

We computed a difference in WPI in response to the Mt. Pinatubo eruption and abrupt quadrupling of $CO_2$ (ΔWPI) to test whether the temperature change in the warm pool is sufficient to explain the difference between the volcanic response and ECS. Consistent with Günther et al. (2022), we find that ΔWPI is positive in most (but not all) models, indicating a greater temperature change in the warm-pool region in response to Pinatubo than in the long-term response to increased $CO_2$ (see Supporting Information S1). A positive ΔWPI is also consistent with the two-layer model generally overestimating the cooling and the volcanic sensitivity from Mt. Pinatubo compared to its CMIP6 counterparts because the prescribed feedbacks in the two-layer model generally aren't negative enough during the short-term response to volcanic forcing. However, because ΔWPI is not correlated with ECS, we should not necessarily expect a correlation between the response to Mt. Pinatubo and ECS.

The constraint on ECS found by Bender et al. (2010) has informed assessments of Earth's ECS such as the most recent IPCC report (Forster et al., 2021). The results of this study show that this constraint is not robust when computed using the much greater quantity of model output available from CMIP6. While useful insights on the climate system can still be gained from analyzing the response to large volcanic eruptions, large-ensembles are needed to interpret the response given the low signal-to-noise ratio of the forced temperature response to internal variability and the climate response to volcanoes is unlikely to be a good analog for the response to anthropogenic greenhouse gas forcing. The results of this study demonstrate the value of large ensembles of climate model simulations in hypothesis testing.

# Geophysical Research Letters

## Data Availability Statement

Details of the CMIP6 models used in this study can be found in Supporting Information S1. The raw CMIP6 data are available at https://esgf-node.llnl.gov/projects/esgf-llnl. Data were downloaded with the scripts from https://doi.org/10.5281/zenodo.4394320 (Loureiro, 2023). The processed CMIP6 data are available at https://doi.org/10.5281/zenodo.7687120 (Pauling, 2023a). The code to reproduce the results is available at https://doi.org/10.5281/zenodo.7687134 (Pauling, 2023b). The CESM2 Large Ensemble data are available at https://www.cesm.ucar.edu/projects/community-projects/LENS2/data-sets.html. The HadCRUT data are available at https://www.metoffice.gov.uk/hadobs/hadcrut5. The ERBE data are available at https://asdc.larc.nasa.gov/project/ERBE%20MEaSUREs/ERBE_S10N_WFOV_SF_ERBS_Regional_Edition4.1.

## References

Barkstrom, B. R. (1984). The earth radiation budget experiment (ERBE). *Bulletin America Meteorology Social*, *65*(11), 1170–1185. https://doi.org/10.1175/1520-0477(1984)065<1170:TERBE>2.0.CO;2

Bender, F. A.-M., Ekman, A. M. L., & Rodhe, H. (2010). Response to the eruption of Mount Pinatubo in relation to climate sensitivity in the CMIP3 models. *Climate Dynamics*, *35*(5), 875–886. https://doi.org/10.1007/s00382-010-0777-3

Caldwell, P. M., Bretherton, C. S., Zelinka, M. D., Klein, S. A., Santer, B. D., & Sanderson, B. M. (2014). Statistical significance of climate sensitivity predictors obtained by data mining. *Geophysical Research Letters*, *41*(5), 1803–1808. https://doi.org/10.1002/2014GL059205

Ceppi, P., & Gregory, J. M. (2019). A refined model for the Earth's global energy balance. *Climate Dynamics*, *53*(7), 4781–4797. https://doi.org/10.1007/s00382-019-04825-x

Dong, Y., Proistosescu, C., Armour, K. C., & Battisti, D. S. (2019). Attributing historical and future evolution of radiative feedbacks to regional warming patterns using a Green's function approach: The preeminence of the western Pacific. *Journal of Climate*, *32*(17), 5471–5491. https://doi.org/10.1175/JCLI-D-18-0843.1

Eyring, V., Cox, P. M., Flato, G. M., Gleckler, P. J., Abramowitz, G., Caldwell, P., et al. (2019). Taking climate model evaluation to the next level. *Nature Climate Change*, *9*(2), 102–110. https://doi.org/10.1038/s41558-018-0355-y

Forster, P. M., Storelvmo, T., Armour, K. C., Collins, W. D., Dufresne, J.-L., Frame, D., et al. (2021). The Earth's energy budget, climate feedbacks, and climate sensitivity. In *Climate change 2021: The physical science basis. Contribution of working group I to the sixth assessment report of the intergovernmental panel on climate change*. Cambridge University Press.

Geoffroy, O., Saint-Martin, D., Olivie, D. J. L., Voldoire, A., Bellon, G., & Tyteca, S. (2013). Transient climate response in a two-layer energy-balance model. Part I: Analytical solution and parameter calibration using CMIP5 AOGCM experiments. *Journal of Climate*, *26*(6), 1841–1857. https://doi.org/10.1175/JCLI-D-12-00195.1

Gregory, J. M., Andrews, T., Ceppi, P., Mauritsen, T., & Webb, M. J. (2020). How accurately can the climate sensitivity to $CO_2$ be estimated from historical climate change? *Climate Dynamics*, *54*(1), 129–157. https://doi.org/10.1007/s00382-019-04991-y

Gregory, J. M., Andrews, T., Good, P., Mauritsen, T., & Forster, P. M. (2016). Small global-mean cooling due to volcanic radiative forcing. *Climate Dynamics*, *47*(12), 3979–3991. https://doi.org/10.1007/s00382-016-3055-1

Gregory, J. M., Ingram, W. J., Palmer, M. A., Jones, G. S., Stott, P. A., Thorpe, R. B., & Williams, K. D. (2004). A new method for diagnosing radiative forcing and climate sensitivity. *Geophysical Research Letters*, *31*(3), L03205. https://doi.org/10.1029/2003GL018747

Günther, M., Schmidt, H., Timmreck, C., & Toohey, M. (2022). Climate feedback to stratospheric aerosol forcing: The key role of the pattern effect. *Journal of Climate*, *35*(24), 4303–4317. https://doi.org/10.1175/JCLI-D-22-0306.1

Hall, A., Cox, P., Huntingford, C., & Klein, S. (2019). Progressing emergent constraints on future climate change. *Nature Climate Change*, *9*(4), 269–278. https://doi.org/10.1038/s41558-019-0436-6

Held, I. M., Winton, M., Takahashi, K., Delworth, T., Zeng, F., & Vallis, G. K. (2010). Probing the fast and slow components of global warming by returning abruptly to preindustrial forcing. *Journal of Climate*, *23*(9), 2418–2427. https://doi.org/10.1175/2009JCLI3466.1

Klein, S. A., & Hall, A. (2015). Emergent constraints for cloud feedbacks. *Current Climate Change Reports*, *1*(4), 276–287. https://doi.org/10.1007/s40641-015-0027-1

Loureiro, T. (2023). tloureiro/cmip6_downloader: 2.0.0. Zenodo. https://doi.org/10.5281/zenodo.4394320

Merlis, T. M., Held, I. M., Stenchikov, G. L., Zeng, F., & Horowitz, L. W. (2014). Constraining transient climate sensitivity using coupled climate model simulations of volcanic eruptions. *Journal of Climate*, *27*(20), 7781–7795. https://doi.org/10.1175/JCLI-D-14-00214.1

Morice, C. P., Kennedy, J. J., Rayner, N. A., Winn, J. P., Hogan, E., Killick, R. E., et al. (2021). An updated assessment of near-surface temperature change from 1850: The HadCRUT5 data set. *Journal of Geophysical Research: Atmosphere*, *126*(3), e2019JD032361. https://doi.org/10.1029/2019JD032361

NASA/LARC/SD/ASDC. (2020). *Earth radiation budget through Earth radiation budget satellite wide-field-of-view nonscanner observations edition 4.1*. NASA Langley Atmospheric Science Data Center DAAC. https://doi.org/10.5067/ERBE/S10N_WFOV_SF_ERBS_Edition4.1

National Research Council. (1979). *Carbon dioxide and climate: A scientific assessment*. The National Academies Press. https://doi.org/10.17226/12181

Nijsse, F. J. M. M., Cox, P. M., & Williamson, M. S. (2020). Emergent constraints on transient climate response (TCR) and equilibrium climate sensitivity (ECS) from historical warming in CMIP5 and CMIP6 models. *Earth System Dynamics*, *11*(3), 737–750. https://doi.org/10.5194/esd-11-737-2020

Pauling, A. G. (2023a). Processed CMIP6 data for "The climate response to the Mt Pinatubo eruption does not constrain climate sensitivity" (v3.0). Zenodo. https://doi.org/10.5281/zenodo.7687120

Pauling, A. G. (2023b). andrewpauling/paulingGRL2022: paulingGRL2022 (v3.0). Zenodo. https://doi.org/10.5281/zenodo.7687134

Pincus, R., Forster, P. M., & Stevens, B. (2016). The radiative forcing model Intercomparison project (RFMIP): Experimental protocol for CMIP6. *Geoscientific Model Development*, *9*(9), 3447–3460. https://doi.org/10.5194/gmd-9-3447-2016

Robock, A. (2000). Volcanic eruptions and climate. *Reviews of Geophysics*, *38*(2), 191–219. https://doi.org/10.1029/1998RG000054

Rodgers, K. B., Lee, S.-S., Rosenbloom, N., Timmermann, A., Danabasoglu, G., Deser, C., et al. (2021). Ubiquity of human-induced changes in climate variability. *Earth System Dynamics*, *12*(4), 1393–1411. https://doi.org/10.5194/esd-12-1393-2021

Rugenstein, M., Bloch-Johnson, J., Gregory, J., Andrews, T., Mauritsen, T., Li, C., et al. (2020). Equilibrium climate sensitivity estimated by equilibrating climate models. *Geophysical Research Letters*, *47*(4), e2019GL083898. https://doi.org/10.1029/2019GL083898

Schmidt, A., Mills, M. J., Ghan, S., Gregory, J. M., Allan, R. P., Andrews, T., et al. (2018). Volcanic radiative forcing from 1979 to 2015. *Journal of Geophysical Research: Atmosphere*, *123*(22), 12491–12508. https://doi.org/10.1029/2018JD028776

Sherwood, S. C., Webb, M. J., Annan, J. D., Armour, K. C., Forster, P. M., Hargreaves, J. C., et al. (2020). An assessment of Earth's climate sensitivity using multiple lines of evidence. *Reviews of Geophysics*, *58*(4), e2019RG000678. https://doi.org/10.1029/2019RG000678

Soden, B. J., Wetherald, R. T., Stenchikov, G. L., & Robock, A. (2002). Global cooling after the eruption of Mount Pinatubo: A test of climate feedback by water vapor. *Science*, *296*(5568), 727–730. https://doi.org/10.1126/science.296.5568.727

Taylor, K. E., Crucifix, M., Braconnot, P., Hewitt, C. D., Doutriaux, C., Broccoli, A. J., et al. (2007). Estimating shortwave radiative forcing and response in climate models. *Journal of Climate*, *20*(11), 2530–2543. https://doi.org/10.1175/JCLI4143.1

Thomason, L. W., Ernest, N., Millán, L., Rieger, L., Bourassa, A., Vernier, J.-P., et al. (2018). A global space-based stratospheric aerosol climatology: 1979–2016. *Earth System Science Data*, *10*(1), 469–492. https://doi.org/10.5194/essd-10-469-2018

Zelinka, M. D., Myers, T. A., Mccoy, D. T., Po-Chedley, S., Caldwell, P. M., Ceppi, P., et al. (2020). Causes of higher climate sensitivity in CMIP6 models. *Geophysical Research Letters*, *47*(1), e2019GL085782. https://doi.org/10.1029/2019GL085782

## References From the Supporting Information

Bethke, I., Wang, Y., Counillon, F., Keenlyside, N., Kimmritz, M., Fransner, F., et al. (2021). NorCPM1 and its contribution to CMIP6 DCPP. *Geoscientific Model Development*, *14*(11), 7073–7116. https://doi.org/10.5194/gmd-14-7073-2021

Boucher, O., Servonnat, J., Albright, A. L., Aumont, O., Balkanski, Y., Bastrikov, V., et al. (2020). Presentation and evaluation of the IPSL-CM6A-LR climate model. *Journal of Advances in Modeling Earth Systems*, *12*(7), e2019MS002010. https://doi.org/10.1029/2019MS002010

Danabasoglu, G., Lamarque, J.-F., Bacmeister, J., Bailey, D. A., DuVivier, A. K., Edwards, J., et al. (2020). The community earth system model version 2 (CESM2). *Journal of Advances in Modeling Earth Systems*, *12*(2), e2019MS001916. https://doi.org/10.1029/2019MS001916

Gutjahr, O., Putrasahan, D., Lohmann, K., Jungclaus, J. H., Storch, J.-S. V., Brüggemann, N., et al. (2019). Max Planck Institute Earth system model (MPI-ESM1.2) for the high-resolution model Intercomparison project (HighResMIP). *Geoscientific Model Development*, *12*(7), 3241–3281. https://doi.org/10.5194/gmd-12-3241-2019

Hajima, T., Watanabe, M., Yamamoto, A., Tatebe, H., Noguchi, M. A., Abe, M., et al. (2020). Development of the MIROC-ES2L Earth system model and the evaluation of biogeochemical processes and feedbacks. *Geoscientific Model Development*, *13*(5), 2197–2244. https://doi.org/10.5194/gmd-13-2197-2020

Hazeleger, W., Severijns, C., Semmler, T., Stefanescu, S., Yang, S., Wang, X., et al. (2010). EC-Earth: A seamless Earth-system prediction approach in action. *Bulletin America Meteorology Social*, *91*(10), 1357–1363. https://doi.org/10.1175/2010BAMS2877.1

Kelley, M., Schmidt, G. A., Nazarenko, L. S., Bauer, S. E., Ruedy, R., Russell, G. L., et al. (2020). GISS-E2.1: Configurations and climatology. *Journal of Advances in Modeling Earth Systems*, *12*(8), e2019MS002025. https://doi.org/10.1029/2019MS002025

Mauritsen, T., Bader, J., Becker, T., Behrens, J., Bittner, M., Brokopf, R., et al. (2019). Developments in the MPI-M Earth system model version 1.2 (MPI-ESM1.2) and its response to increasing $CO_2$. *Journal of Advances in Modeling Earth Systems*, *11*(4), 998–1038. https://doi.org/10.1029/2018MS001400

Sellar, A. A., Jones, C. G., Mulcahy, J. P., Tang, Y., Yool, A., Wiltshire, A., et al. (2019). UKESM1: Description and evaluation of the U.K. Earth system model. *Journal of Advances in Modeling Earth Systems*, *11*(12), 4513–4558. https://doi.org/10.1029/2019MS001739

Swart, N. C., Cole, J. N. S., Kharin, V. V., Lazare, M., Scinocca, J. F., Gillett, N. P., et al. (2019). The Canadian earth system model version 5 (CanESM5.0.3). *Geoscientific Model Development*, *12*(11), 4823–4873. https://doi.org/10.5194/gmd-12-4823-2019

Tatebe, H., Ogura, T., Nitta, T., Komuro, Y., Ogochi, K., Takemura, T., et al. (2019). Description and basic evaluation of simulated mean state, internal variability, and climate sensitivity in MIROC6. *Geoscientific Model Development*, *12*(7), 2727–2765. https://doi.org/10.5194/gmd-12-2727-2019

Voldoire, A., Saint-Martin, D., Senesi, S., Decharme, B., Alias, A., Chevallier, M., et al. (2019). Evaluation of CMIP6 DECK experiments with CNRM-CM6-1. *Journal of Advances in Modeling Earth Systems*, *11*(7), 2177–2213. https://doi.org/10.1029/2019MS001683

Volodin, E. M., Mortikov, E. V., Kostrykin, S. V., Galin, V. Y., Lykossov, V. N., Gritsun, A. S., et al. (2017). Simulation of the present-day climate with the climate model INMCM5. *Climate Dynamics*, *49*(11), 3715–3734. https://doi.org/10.1007/s00382-017-3539-7

Yukimoto, S., Kawai, H., Koshiro, T., Oshima, N., Yoshida, K., Urakawa, S., et al. (2019). The Meteorological Research Institute Earth System Model version 2.0, MRI-ESM2.0: Description and basic evaluation of the physical component. *Journal of the Meteorological Society of Japan. Ser. II*, *97*(5), 931–965. https://doi.org/10.2151/jmsj.2019-051

Ziehn, T., Chamberlain, M. A., Law, R. M., Lenton, A., Bodman, R. W., Dix, M., et al. (2020). The Australian earth system model: ACCESS-ESM1.5. *Journal of Southern Hemisphere Earth Systems Science*, *70*(1), 193–214. https://doi.org/10.1071/ES19035